

FRICTION EVALUATION OF LASER TEXTURED TOOL STEEL SURFACES

Jana ŠUGÁROVÁ*, Peter ŠUGÁR*, Martin FRNČÍK*

*Slovak University of Technology, Faculty of Material Science and Technology, Institute of Production Technologies,
J. Bottu 25, 917 24 Trnava, Slovakiajana.sugarova@stuba.sk, peter.sugar@stuba.sk, martin.frcnik@stuba.sk

received 2 November 2015, revised 12 May 2017, accepted 17 May 2017

Abstract: Surface textures can be defined as a regularly arranged micro-depressions or grooves with defined shape and dimensions. These textures, if they are manufactured by laser ablation process, contribute to a significant improvement of the tribological, optical or various biological properties. The aim of this paper is to analyze the influence of the surface textures prepared by laser surface texturing (LST) at the friction coefficient value measured on the tool (90MnCrV8 steel) – workpiece (S235JRG1 steel) interface. Planar frontal surfaces of compression platens have been covered by parabolic dimple-like depressions with different dimensions. The morphological analysis of such manufactured depressions has been performed by laser scanning microscopy. Influence of such created textures on the tribological properties of the contact pair has been analyzed by the ring compression test method in the terms of hydrodynamic lubrication regime. The experimental research shown that by applying of surface textures with defined shape and dimensions and using an appropriate liquid lubricant at the same time, the coefficient of contact friction can be reduced nearly to the half of its original value.

Key words: Laser Surface Texturing, Dimple-Like Depressions, Friction Coefficient, Lubrications, Ring – Test

1. INTRODUCTION

Steels are representative structural materials for most mechanical applications because of their high strength and toughness, good machinability and relatively low cost. Surface hardness and chemical composition of applied coating play a dominant role against wear under sliding conditions. The efficiency, reliability, and durability of mating mechanical components depend on friction occurring at the interface during the sliding (Gualtieri et al., 2009). The surface texture and geometry are the key factors which determine the functionality of the surface. The idea of using surface texturing for improving tribological performance is not a new development (Ibatan et al., 2015). A general classification on the methods to produce surface texture can be made as bottom to top and top to bottom (Demir et al., 2013). The methods involving bottom to top strategies are the ones, where the surface is usually deposited with chemical/physical process in the form of a coating or surface is generated layer by layer. The dimensional scale of the patterns can reach the nanometric level. On the other hand, top to bottom methods based on material removal from an initial surface are potentially more flexible. Top to bottom methods involve techniques such as grinding and honing (Jeng, 1996), chemical etching (Rech et al., 2002), electron ion etching (Zhu et al., 2003), electric-discharge machining (Aspinwall et al., 1996), laser beam machining (Etsion, 2005), micro-casting (Cannon and King, 2009) and micro-ball end milling (Yan et al., 2010).

According to the Ibatan et al. (2015) LST is one of the most advanced techniques in producing of micro-dimple patterns for sliding contacts. The laser used is extremely fast, allowing short processing times. It provides high precision control of the size and shape, enabling the construction of optimized geometrical parameters and can be used for a wide range of materials including metals, ceramics and polymers. The texturing process involves focused pulsed laser to produce micro-dimple patterns surround-

ed by a solidified melt rim. Due to high energy involved with LST, material melting and vaporization occur, leading to heat affected zones (HAZ) on the solidified melt rim, and hence changing the local microstructures and mechanical properties. To minimize the microstructural changes and size of solidified melt rim, appropriate pulse energy and pulse frequency can be modified (Vilhena et al., 2009). Lasers commonly used on LST are CO₂ and Nd:YAG (Schaeffer, 2012). Currently, laser systems applied in production of surface textures operates with pulse duration at the femtosecond level (Štašić, 2011).

The use of a laser beam allows direct writing of the texture patterns, use of masks (Ortabasi et al., 1997), or diffractive optics (Huang et al., 2010) to generate patterns on the surface. Direct writing with the laser beam is the most flexible among the listed, since the same optical chain can be manipulated to work on different materials and patterns. A single tool for flexible machining conditions which can be adapted to different applications is an attractive solution for industrial use (Demir et al., 2013).

Surface texturing can be obtained by protrusions or dimples. Dimple configuration is more popular, especially in elasto-hydrodynamic and boundary lubrication regimes. For protruded surface texturing, contact area between the surface and the protruded geometry is much larger in comparison with dimpled surface, resulting in higher average contact pressure and higher wear rates (Ibatan et al., 2015). The aim of micro-texturing is either to increase or to decrease friction (Braun et al., 2014). Textures, like channels or crossed channels are reported to do both, increase (Zum Gahr et al., 2009; Wahl et al., 2012) or decrease (Costa and Hutchings, 2009) friction, depending on the tribological conditions. Furthermore, for textures like dimples the effect to reduce friction is reported, especially under hydrodynamic lubrication conditions (Etsion, et al., 1999; Etsion, 2005). Four mechanisms are postulated in the literature, which might lead to the reduction in friction and wear by micro-dimples: (i) the trapping of wear debris (Varen-

berg et al., 2002), (ii) changes in the contact angle (Ma et al., 2013), (iii) the storage of lubricant (Lu and Khonsari, 2007) and (iv) a micro-hydrodynamic pressure build-up (Scaraggi, 2012).

The geometry and dimensions of surface texture vary in shapes and sizes from a few microns to hundreds of microns. Typical texture shapes (protruded and recessed) involved are circular, square, triangle, and hexagon, but different patterns of microgrooves are also studied (Ibatan et al., 2015). Circular dimple-like depressions are still the most commonly used geometrical pattern due to their easy fabrication and low cost (Yan et al., 2010). There are three major parameters involved with surface texturing, such as dimple shape, dimple depth and dimple density (Ma and Zhu, 2011; Ronen et al., 2001). By considering all the geometric parameters, texture shapes are optimized to achieve the optimum shapes which will provide the best tribological performance in terms of minimum friction and maximum load carrying capacity (Sheen and Khonsari, 2015; Qiu et al., 2013). It has been found that the optimum geometry for each shape is not identical but similar, and the regular shape such as ellipse with round or curved edge is shown to reduce the friction and increase load carrying capacity significantly as compared to other shapes (Ibatan et al., 2015). Fig. 1 demonstrates important geometries of a surface texture and regular texture shapes currently studied by researchers. Except the above mentioned parameters, geometries such as bottom shape profile, orientation of surface texture to sliding direction, and cellular arrangement of surface texture are counted in key texture parameters too. It is emphasized that surface texturing may have negative effects on the tribological performance of a sliding couple if the surface texture is not optimized (Mourier et al., 2006).

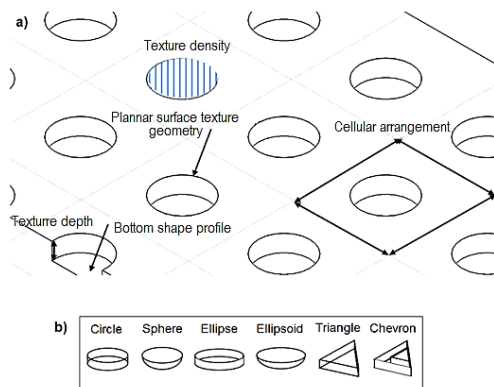


Fig. 1. Surface texture geometry; (a) key geometrical parameters of a surface texture, (b) shapes of dimples (Ibatan et al., 2015)

The applications of LST encompass the ones requiring improved tribological (Etsion, 2005), biomedical (Samad-Zadeh et al., 2011), and optical (Iyengar et al., 2011) properties; as well as control of surface wetting (Bizi-Bandoki et al., 2011), and improvement of adhesion joint strength (Man et al., 2010). Various pulsed laser systems operating in different pulse regimes with wavelengths varying from IR to UV are employed for different texturing applications (Schaeffer, 2012).

2. EXPERIMENTAL SETUP

The aim of this paper is to analyze the influence of the surface textures prepared by LST on the friction coefficient value, which

was measured at the tool – workpiece interface. Contact pair consists of a pair of compression platens (upper and lower one); among them the test sample is axially compressed. Frontal areas of each compression platen have been covered by a texture of defined shape and dimensions. There were used a four pairs of compression platens in the experiment; their frontal areas were modified by regularly arranged micro-dimples:

(A) dimples with a diameter of 100 μm and a depth of 10 μm produced by hatching machining strategy,

(B) dimple diameter of 100 μm and the depth of 10 μm produced by caving machining strategy,

(C) dimple diameter of 100 μm and the depth of 40 μm produced by hatching machining strategy and

(D) dimple diameter of 100 μm and the depth of 40 μm produced by caving machining strategy.

Surface density of the studied textures makes approximately 6%. Each texture consists of dimple-like depressions with a diameter of a 100 μm . Depressions are situated at the corners of the regular hexagon with a side length of 400 μm . One depression is placed into the center of this formation, as demonstrates Fig. 2a. Fig. 2b illustrates an ideal profile of depression of both studied depth (10 μm and 40 μm).

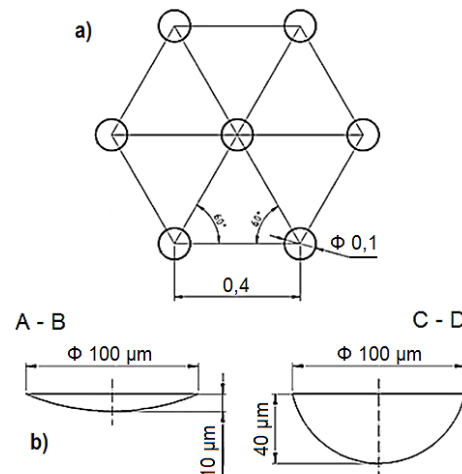


Fig. 2. Studied textures; (a) deployment of depressions in the basic formation; (b) ideal profile of studied depressions

Compression platens were manufactured of 90MnCrV8 steel according to EN ISO 4957, since this type of material is widely applied in production of blank metal forming tools. Chemical composition of this tool steel is specified in Tab. 1. Hardening of manufactured tools to desired hardness of 53 – 55 HRC had gone before the production of defined textures on the frontal areas of these tools. Subsequently, the frontal areas were grinded to obtain a surface roughness (R_a) of 0.4 μm , then textured by laser beam.

To manufacture surface textures on the frontal areas of compression plates a 5-axis high precision laser machining centre LASERTEC 80 Shape has been used. This machine is equipped with a pulsed fiber Nd:YAG laser with a wavelength of 1064 nm. Tab. 2 contains a description of the laser beam parameters used to produce the surface textures. These parameters had been optimized in order to a depth of cut of 1 μm per a layer was achieved.

Tab. 1. Chemical composition of tool steel (Preciz, 2012)

C [wt %]	Si [wt %]	Mn [wt %]	P _{max} [wt %]	S _{max} [wt %]	Cr [wt %]	V [wt %]
0.85 -0.95	0.10 - 0.40	1.90 - 2.10	0.030	0.030	0.20 -0.50	0.05 -0.15

Tab. 2. Parameters of laser beam utilized to production of micro-dimples

Parameter	Value
Power P (W)	10.075
Scanning speed v_s (mm/s)	1200
Repetition rate (kHz)	60
Pulse duration t_p (ns)	120

Fig. 3 demonstrates the result of laser beam machining process – tool for compression test whose frontal area is covered by texture D. Total textured area makes 256 mm² (a square with a side length of 16 mm).

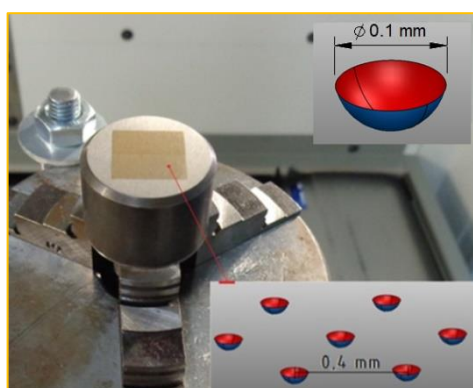


Fig. 3. Tool for compression test with frontal area covered by texture D

In order to determine the real shape and dimensions of such manufactured surface depressions a morphological analysis has been performed. This analysis of chosen depression of each surface texture's type has been performed using a laser confocal microscope Zeiss LSM 700 (with resolution of 0.12 μm). Fig. 4 shows a real 3D shapes and dimensions of analyzed dimples of each studied texture, which were manufactured by two different machining strategies.

The same figure shows that around the edge of each depression a rim of solidified melt was created. This rim is a typical element of the structures manufactured by laser beam in a material ablation processes. More or less, this negative effect can be minimized by optimizing the parameters of laser beam with a subsequent polishing of textured surfaces.

To determine the friction coefficient of the contact pair a ring compression test was performed. During this test a ring-shaped test sample is axially compressed among the pair of compression platens; test samples were manufactured of S235JRG1 steel (EN 10027-1). Chosen steels represent and simulate the contact materials (forming tool and the formed component) of the real specific metal forming process. Tab. 3 documents the chemical composition of material of test samples. This test is based on the assumption that the friction coefficient is constant at the whole contact surface and the deformation of the test ring is homogeneous. During this compression, the hole diameter of the test sample

can be reduced, remain without a change or even increased (depending on the size of the friction coefficient). When the test sample is compressed in frictionless conditions, the hole diameter increases proportionally with the increase of the outer diameter. With the friction growth the increase of hole diameter is hampered and at a certain size of radial pressure this diameter can be reduced (Plančak, 2012). The ratio of outer diameter to the hole diameter to the height of test sample $D : d : h$ is equal to 6 : 3 : 2. The dimensions of test samples are typically 12 mm : 6 mm : 4 mm according to this ratio. Frontal areas of test samples were non-textured; what is more, these surfaces had been grinded to obtain a required surface roughness (R_a) of 0.4 μm. It is important to preserve approximately an equal compression of test sample ΔH during the test; its value should be in the interval from 0.2 to 0.5 mm.

Tab. 3. Chemical composition of test samples (CZ Ferro-Steel, 2011)

C _{max} [wt %]	Mn [wt %]	Si [wt %]	P _{max} [wt %]	S _{max} [wt %]	N _{max} [wt %]	Al [wt %]
0.17	-	-	0.045	0.045	0.007	-

Tab. 4. Physical and chemical properties of applied liquid lubricants

Variocut C 462	
A high performance and heavy-metal free neat cutting oil.	
Physical and chemical properties	
Appearance	yellow liquid
Viscosity at 40 °C (mm ² /s)	22 (according DIN 51 562)
Density 15 °C (kg/m ³)	908 (DIN 51 757)
Flash point (°C)	164 (ISO 2592)
Iloform FST 4	
A medium viscosity, neat forming oil containing high levels of advanced lubricity and extreme pressure additives. It is free of chlorine and heavy metals (such as Barium).	
Physical and chemical properties	
Appearance	dark brown liquid
Viscosity at 40 °C (mm ² /s)	120 (according to DIN 51 562)
Density at 20 °C (kg/m ³)	< 1000 (DIN 51 757)
Flash point (°C)	144 (ISO 2592)

Friction coefficient evolution was recorded in a hydrodynamic lubrication regime; two types of liquid lubricants were used to ensure this “full lubrication” configuration at the contact interface: a mineral VarioCut C462 oil and Iloform FST4 oil, physical and chemical properties of applied lubricants are depicted in Tab. 4. Both non-textured and textured compression platens were tested for comparison.

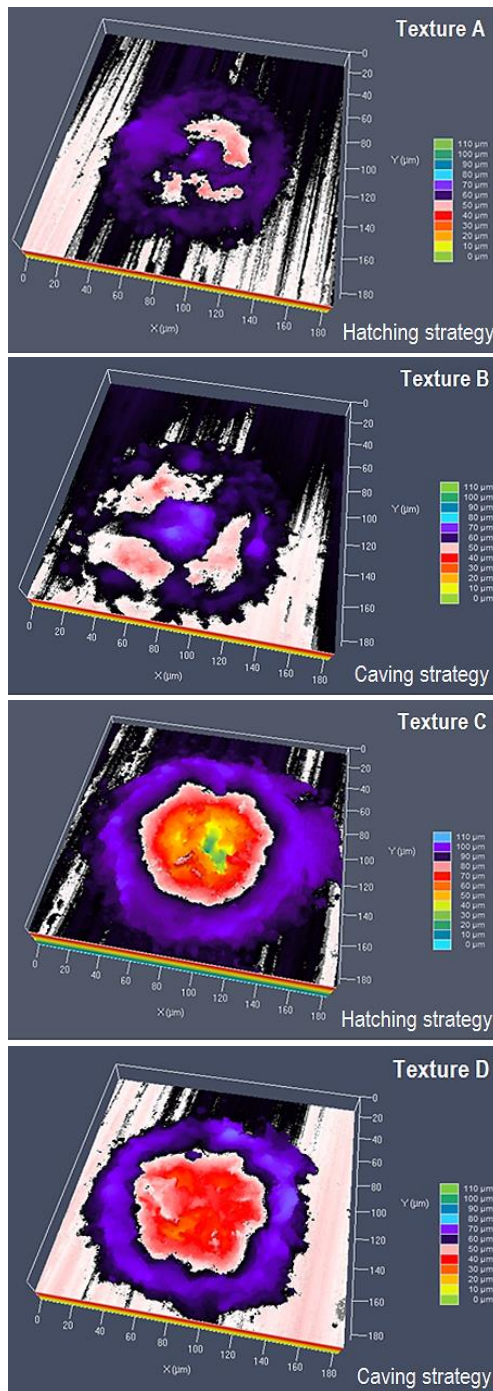


Fig. 4. Real 3D shapes of chosen depression of each studied surface textures

3. RESULTS AND DISCUSSION

Single friction coefficients obtained through a ring compression test, measured in various combination of surface texture with/without a lubricant, are specified in Tab. 5. Two test samples (8 test samples compressions) have been used for analysis of each combination of input parameters from Tab. 5. Reference value (shown in red) is represented by experiment no. 13; contact surfaces were non-textured in lubrication-free friction regime, friction coefficient f_{13} got at 0.275 ± 0.015 value. This value is in accordance with the Engineering ToolBox (2014); where the

friction coefficient attains value from 0.25 to 0.8 for a steel – steel contact pair.

Tab. 5. Design of experiment and obtained friction coefficients

Experiment	Texture	Lubricant	Coefficient of friction (-)
1.	A	-	0.18 ± 0.013
2.		Variocut C462	0.18 ± 0.005
3.		Iloform FST 4	0.21 ± 0.010
4.	B	-	0.26 ± 0.010
5.		Variocut C462	0.22 ± 0.005
6.		Iloform FST 4	0.22 ± 0.012
7.	C	-	0.26 ± 0.013
8.		Variocut C462	0.23 ± 0.014
9.		Iloform FST 4	0.18 ± 0.001
10.	D	-	0.25 ± 0.010
11.		Variocut C462	0.16 ± 0.009
12.		Iloform FST 4	0.15 ± 0.001
13.	-	-	0.275 ± 0.015

Friction coefficients values are depicted in Fig. 5 in relation to the reference value. In all executed experiments friction coefficients reached a lower value than the reference value (if the values of standard deviations are neglected). There are an individual friction conditions distinguished by a color in this figure (grey shades for lubricant-free regime, green shades for Variocut C 462 and blue shades for Iloform FST 4). The influence of defined surface textures on the friction coefficient value in lubrication-free regime is meaningless in the experiments no. 4 (friction reduction of only 5.5 %), no. 7 (friction reduction of only 5.5 %) and no. 10 (friction reduction of 9.1 %), because the friction coefficient values in these experiments are similar to the reference value. It means, these defined surface textures do not contribute to reducing the friction coefficient at the analyzed tool - workpiece interface in the lubrication-free regime. The exception has been observed in the experiment no. 1, when applied surface texture contributed to the reduction of friction, friction coefficient value decreased to $f_1 = 0.18$ (35 % friction reduction compared to the reference value).

Horizontally hatched columns in Fig. 5 demonstrate the friction coefficient values obtained in the experiments where the Variocut C462 lubricant has been used to ensure the hydrodynamic friction regime. The largest reduction of friction has been observed in the experiment no. 11 (Texture D + Variocut C462) with the friction coefficient value of 0.16 (42 % friction reduction). Friction reduction has been successfully observed in other experiments too – experiment no. 2 with the friction coefficient value $f_2 = 0.18$ (35 % friction reduction), which is substantially the same value as in the experiment no. 1 (surface texture A in lubrication-free regime, $f_1 = 0.18$); which means, applied liquid lubricant does not contribute to reducing of friction, reducing of friction coefficient is probably achieved by applying of surface Texture A. In experiment no. 5 friction coefficient of 0.22 has been measured and in experiment no. 8 the friction coefficient 0.233 has been observed (friction reduction of 20 %, resp. of 16.4 %).

Double diagonally hatched columns in Fig. 5 depict the friction coefficient values obtained in the experiments where the Iloform FST4 lubricant has been used. During the ring compression test execution an undesirable phenomenon was observed – there was

a high adhesion of test sample to the upper compression platen. This phenomenon came into existence as a result of high lubricant viscosity (see Tab. 4). A combination of surface Texture D with

liquid lubricant Iloform FST 4 in experiment no. 12 achieved the lowest friction coefficient value ($f_{12} = 0.15$) of all performed experiments (46 % friction reduction).

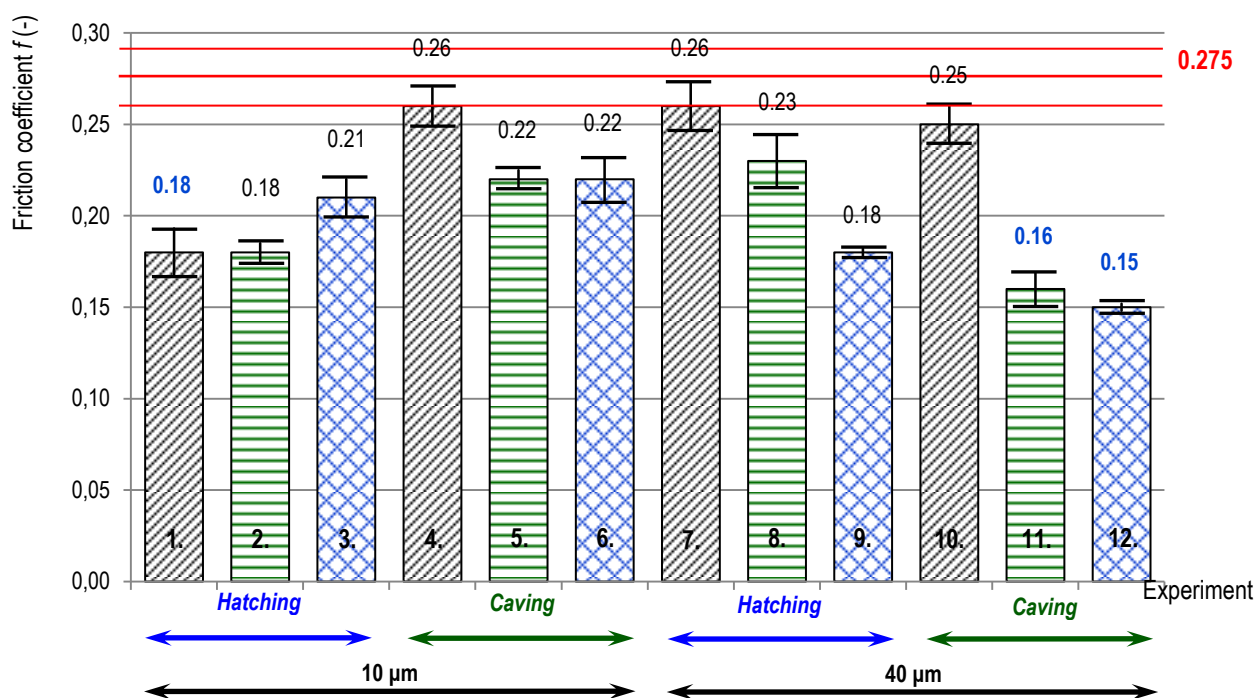


Fig. 5. Graphical comparison of obtained friction coefficients in a relation to the reference value

Tab. 6. Friction coefficient values relative to the defined surface texture and applied liquid lubricant

	Texture A	Texture B	Texture C	Texture D	Reference sample	Friction reduction
No lubricant	0.18	0.26	0.26	0.25	0.275	35 %
Variocut C462	0.18	0.22	0.23	0.16		42 %
Iloform FST4	0.21	0.22	0.18	0.15		46 %

The machining strategy is an important factor that significantly affects the desired shape and dimensional accuracy of produced surface dimple-like depressions. The influence of machining strategy on the tribological properties of contact surfaces (friction coefficient in particular) is observed for both types of textures and all tribological regimes. If a shape and dimensional accuracy of Texture C (hatching strategy) and Texture D (caving strategy) is compared, we can see that hatching machining strategy contributed to the production of shape and dimensionally more accurate depressions than in caving strategy, but the better tribological behaviour has been observed in Texture D (when both lubricants were applied). The reason is that by caving machining strategy a more favorable dimple diameter to the dimple height ratio d_p/h_p was achieved (in this case the value of the ratio is circa 0.18), whereas the value of the ratio is circa 0.32 for Texture C. The optimal value of the ratio can be found in the interval from 0.1 to 0.2, according to Ronen et al. (2001).

Tab. 6 demonstrates the friction coefficient values relative to the reference value when various surface textures and lubricants were applied to modify the tribological conditions of contact sur-

faces. There are also marked the lowest friction coefficient values which were measured in single friction conditions.

4. CONCLUSION

According to Tang et al. (2013) surface texturing is a widely used approach to improve the load capacity, the wear resistance, and the friction coefficient of tribological mechanical components. Laser surface texturing with a parabolic dimple-like depressions with depths of 10 μ m and 40 μ m and diameter of 100 μ m and a textured area of 6 % has been applied to 90MnCrV8 steel frontal area in order to analyze the influence on the friction coefficient measured at the tool – workpiece interface. Laser texturing has been performed using a pulsed fiber Nd:YAG laser with pulse duration of 120 ns. Two different machining strategies were applied in production of surface textures in order to find which strategy produces shape and dimensionally more precise micro-dimples. The morphological characterization of ablated surfaces has been performed using laser confocal microscopy technique. Tribological tests have been performed in hydrodynamic lubrication configuration, where two different types of liquid lubricants were applied at room temperature.

Results confirmed the influence of machining strategy on the geometrical parameters of produced dimples and the impact on friction behavior of the surface. Also significant improvement of friction behavior under lubricate conditions has been observed. Textured contact surface modified by Iloform FST4 lubricant showed better friction behavior than reference surface. Reference value corresponding to a non-treated surface was established at 0.275 ± 0.015 . Friction coefficient was in this case reduced to 0.15 value (the best friction coefficient reduction of 46 %), which

means, that by applying of surface textures with defined shape and dimensions and using an appropriate liquid lubricant at the same time, the coefficient of contact friction can be reduced nearly to the half of its original value. The surface texturing is important in reducing friction and wear. The generation of hydrodynamic pressure, the function of micro-trap for wear debris, and the micro-reservoirs for lubricant retention are the main mechanisms responsible for reducing the friction and wear in this method of surface treatment.

Presented results give answer on the questions regarding the influence of laser texture machining parameters and lubrication of laser textured surfaces on the friction behavior. In the experiments only planar surfaces have been evaluated. More complicated situation arises in the case where a complex shaped surface is used.

REFERENCES

1. **Aspinwall D.K., Wise M.L.H., Stout K.J. et al.** (1996), Electrical discharge texturing, *Int. Journal of Machine Tools & Manufacture*, 32(1-2), 183-193.
2. **Bizi-Bandoki P., Benayoun S., Valette S. et al.** (2011), Modifications of roughness and wettability properties of metals induced by femtosecond laser treatment, *Applied Surface Science*, 257(12), 5213-5218.
3. **Braun D., Greiner Ch., Schneider J. et al.** (2014), Efficiency of laser surface texturing in the reduction of friction under mixed lubrication, *Tribology International*, 77, 142-147.
4. **Cannon A.H., King W.P.** (2009), Casting metal microstructures from a flexible and reusable mold, *Journal of Micromechanics and Microengineering*, 19, 1-6.
5. **Costa H.L., Hutchings I.M.** (2009), Effects of die surface patterning on lubrication in strip drawing, *Journal of Materials Processing Technology*, 209(3), 1175-1180.
6. **CZ Ferro-Steel** (2011), ČSN 11373 – non-alloy steel for construction purposes (<http://www.czferrosteel.cz/pdf/tyce-11373.pdf>)
7. **Demir A.G., Maressa P., Previtali B.** (2013), Fibre laser texturing for surface functionalization, *Physics Procedia*, 41, 759-768.
8. **Etsion I.** (2005), State of the art in laser surface texturing, *Journal of Tribology*, 127(1), 248-253.
9. **Etsion I., Kligerman Y., Halperin G.** (1999), Analytical and experimental investigation of laser-textured mechanical seal faces, *Tribology Transactions*, 42(3), 511-516.
10. **Gualtieri E., Borghi A., Calabri L. et al.** (2009), Increasing nano-hardness and reducing friction of nitride steel by laser surface texturing, *Tribology International*, 42(5), 699-705.
11. **Huang J., Beckemper S., Gillner A. et al.** (2010), Tunable surface texturing by polarization-controlled three-beam interference, *Journal of Micromechanics and Microengineering*, 20(9), p. 095004.
12. **Ibatan T., Uddin M.S. and Chowdury M.A.K.** (2015), Recent development on surface texturing in enhancing tribological performance of bearing sliders, *Surface & coatings Technology*, 272, 102-120.
13. **Iyengar V.V., Nayak B.K., Gupta M.C.** (2011), Ultralow reflectance metal surfaces by ultrafast laser texturing, *Applied Optics*, 49(31), 5983-5988.
14. **Jeng Y-R.** (1996), Impact of Plateaued Surfaces on Tribological Performance, *Tribology Transactions*, 39(2), 354-361.
15. **Lu X., Khonsari M.M.** (2007), An experimental investigation of dimple effect on the Stribeck curve of journal bearings, *Tribology Letters*, 27(2), 169-176.
16. **Ma Ch., Bai S., Peng X. et al.** (2013), Improving hydrophobicity of laser textured SiC surface with micro-square convexes, *Applied Surface Science*, 266(1), 51-56.
17. **Ma Ch., Zhu H.** (2011), An optimum design model for textured surface with elliptical-shape dimples under hydrodynamic lubrication, *Tribology International*, 44(9), 987-995.
18. **Man H.C., Chiu K.Y., Guo X.** (2010), Laser surface micro-drilling and texturing of metals for improvement of adhesion joint strength, *Applied Surface Science*, 256(10), 3166-3169.
19. **Mourier L., Mazuyer D., Lubrecht A.A. et al.** (2006), Transient increase of film thickness in micro-textured EHL contacts, *Tribology International*, 39(12), 1745-1756.
20. **Ortabasi U., Meier D.L., Easoz J.R. et al.** (1997), Excimer micromachining for texturing silicon solar cells, *Lasers As Tools For Manufacturing II*, SPIE Press, 54-64.
21. **Plančák M., Kostka P., Schrek A.** (2012), *Dictionary of metal forming*, Nakladatelstvo STU, Bratislava.
22. **Preciz** (2012), 1.2842 (90MnCrV8, 19 312 / 19 313), <http://www.preciz.cz/sluzby-hlavni/material-normal/1.2842>)
23. **Qiu M., Minson B., Raeymaekers B.** (2013), The effect of texture shape on the friction coefficient and stiffness of gas-lubricated parallel slider bearings, *Tribology International*, 67, 278-288.
24. **Rech B., Kluth O., Repmann T. et al.** (2002), New materials and deposition techniques for highly efficient silicon thin film solar cells, *Solar Energy Materials and Solar Cells*, 74(1-4), 439-447.
25. **Ronen A., Etsion I., Kligerman Y.** (2001), Friction-reducing surface-texturing in reciprocating automotive components, *Tribology Transactions*, 44(3), 359-366.
26. **Samad-Zadeh A., Harsono M., Belikov A. et al.** (2011), The influence of laser-textured dental surface on bond strength, *Dental Materials*, 27(10), 1038-1044.
27. **Scaraggi M.** (2012), Textured surface hydrodynamic lubrication: Discussion, *Tribology Letters*, 48(3), 375-391.
28. **Schaeffer R.D.** (2012), *Fundamentals of laser micromachining*, CRC Press. London.
29. **Shen C. and Khonsari M.M.** (2015), Numerical optimization of texture shape for parallel surfaces under unidirectional and bidirectional sliding, *Tribology International*, 82, 1-11.
30. **Staić J., Gaković B., Perrie W. et al.** (2011), Surface texturing of the carbon steel AISI 1045 using femtosecond laser in single pulse and scanning regime, *Applied Surface Science*, 258(1), 290-296.
31. **Tang W., Zhou Y., Zhu H. et al.** (2013), The effect of surface texturing on reducing the friction and wear of steel under lubricated sliding contact, *Applied surface science*, 273, 199-204.
32. **Engineering ToolBox** (2014), *Friction and coefficients of friction*, (http://www.engineeringtoolbox.com/friction-coefficients-d_778.html)
33. **Varenberg M., Halperin G., Etsion I.** (2002), Different aspects of the role of wear debris in fretting wear, *Wear*, 252(11-12), 902-910.
34. **Vilhena L.M., Sedláček M., Podgornik B. et al.** (2009), Surface texturing by pulsed Nd:YAG laser, *Tribology International*, 42(10), 1496-1504.
35. **Wahl R., Schneider J., Gumbsch P.** (2012), Influence of the real geometry of the protrusions in microtextured surfaces on frictional behaviour, *Tribology Letters*, 47(3), 447-453.
36. **Yan J., Zhang Z., Kuriyagawa T. et al.** (2010), Fabricating microstructured surface by using single-crystalline diamond endmill, *Int. Journal of Advanced Manufacturing Technology*, 51, 957-964.
37. **Zhu X.P., Lei M.K., Ma T.C.** (2003), Surface morphology of titanium irradiated by high-intensity pulsed ion beam, *Nuclear Instruments & Methods in Physics Research Section B: Beam Interactions with Materials and Atoms*, 211(1), 69-79.
38. **Zum Gahr K.H., Wahl R., Wauthier K.** (2009), Experimental study of the effect of microtexturing on oil lubricated ceramic/steel friction pairs, *Wear*, 267(5-8), 1241-1251.

Acknowledgement: This work was supported by the research project, entitled: Innovative methods of sheet metal forming tools surfaces improvement - R&D (Manunet 2014/11283); and VEGA project: Laser surface texturing technology research for an optimizing of tribological conditions in the sheet metal forming processes (0669/15).